Article

Cell Reports

# PROS-1/Prospero Is a Major Regulator of the Glia-Specific Secretome Controlling Sensory-Neuron Shape and Function in *C. elegans*

## Graphical Abstract

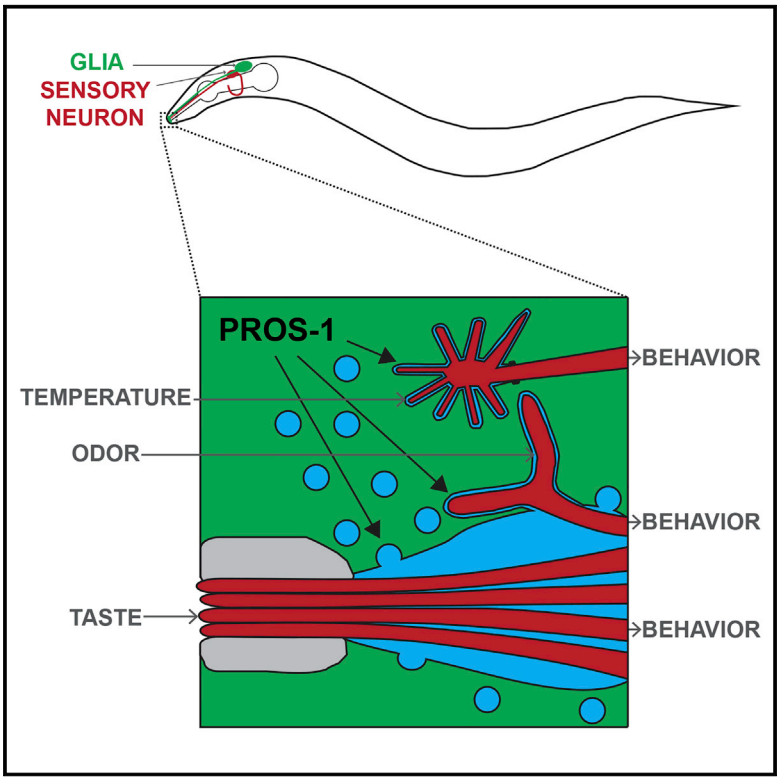


## Authors

Sean W. Wallace, Aakanksha Singhvi, Yupu Liang, Yun Lu, Shai Shaham

## Correspondence

shaham@rockefeller.edu

## In Brief

Wallace et al. find a post-developmental role for the transcription factor *pros-1*/Prospero in regulating expression of glia-secreted proteins and controlling the morphology and function of glia-associated neurons. *pros-1* homologs are expressed in differentiated glia in vertebrates and may play similar roles in regulating glia-neuron interactions.

## Highlights

- *C. elegans* glia expression profiling identifies many post-embryonically secreted proteins
- The transcription factor *pros-1*/Prospero functions post-developmentally in glia
- *pros-1* controls expression of genes encoding secreted/membrane proteins
- *pros-1* acting through its targets controls morphology/function of associated neurons

Wallace et al., 2016, Cell Reports *15*, 550–562
April 19, 2016 
http://dx.doi.org/10.1016/j.celrep.2016.03.051

CellPress

OPEN ACCESS
CellPress

Cell Reports
Article

# PROS-1/Prospero Is a Major Regulator of the Glia-Specific Secretome Controlling Sensory-Neuron Shape and Function in *C. elegans*

Sean W. Wallace,[1] Aakanksha Singhvi,[1] Yupu Liang,[2] Yun Lu,[1] and Shai Shaham[1,*]
[1]Laboratory of Developmental Genetics, The Rockefeller University, 1230 York Avenue, New York, NY 10065, USA
[2]CCTS Research Bioinformatics, The Rockefeller University, 1230 York Avenue, New York, NY 10065, USA
*Correspondence: shaham@rockefeller.edu
http://dx.doi.org/10.1016/j.celrep.2016.03.051

## SUMMARY

**Sensory neurons are an animal's gateway to the world, and their receptive endings, the sites of sensory signal transduction, are often associated with glia. Although glia are known to promote sensory-neuron functions, the molecular bases of these interactions are poorly explored. Here, we describe a post-developmental glial role for the PROS-1/Prospero/PROX1 homeodomain protein in sensory-neuron function in *C. elegans*. Using glia expression profiling, we demonstrate that, unlike previously characterized cell fate roles, PROS-1 functions post-embryonically to control sense-organ glia-specific secretome expression. PROS-1 functions cell autonomously to regulate glial secretion and membrane structure, and non-cell autonomously to control the shape and function of the receptive endings of sensory neurons. Known glial genes controlling sensory-neuron function are PROS-1 targets, and we identify additional PROS-1-dependent genes required for neuron attributes. *Drosophila* Prospero and vertebrate PROX1 are expressed in post-mitotic sense-organ glia and astrocytes, suggesting conserved roles for this class of transcription factors.**

## INTRODUCTION

Animals use specialized sense organs to obtain information from their environment. Sense organs, in general, consist of sensory neurons or receptor cells, the primary mediators of sensory signal transduction, and glia-like support cells, which have been defined anatomically for decades but have been relatively poorly studied (Cuschieri and Bannister, 1975; Engström, 1967; Murray, 1993). Glia-like cells in the mammalian taste bud, olfactory epithelium, cochlea, and retina, classified as type I cells, sustentacular cells, Deiters' cells, and RPE (retinal pigment epithelial) cells, respectively, show a number of functions typically associated with glia. These include regulating neurotransmitter signaling (Bartel et al., 2006; Dooley et al., 2011; Hegg et al., 2009; Lawton et al., 2000; Matsunobu et al., 2001), buffering extracellular potassium levels (Boettger et al., 2002; Dvoryanchikov et al., 2009; Trotier, 1998), and releasing neurotrophic factors and neuromodulators (Breunig et al., 2010; Hansel et al., 2001; Strauss, 2005). Thus, functional similarities between sense-organ and CNS glia, and similarities between sensory-neuron receptive endings and synapses (Shaham, 2010), suggest that understanding sensory neuron-glia interactions may have broad relevance.

*C. elegans* is an attractive model system for studying glia-neuron interactions (Oikonomou and Shaham, 2011; Shaham, 2006, 2015). Its simple anatomy, facile genetics, optical transparency, and well-characterized behavioral responses allow for single-cell-resolution in vivo analyses of the contributions that glial cells make to nervous system function. The *C. elegans* amphids are a pair of bilaterally symmetric head sense organs that mediate responses to multiple sensory inputs (Bargmann et al., 1993; Bargmann and Horvitz, 1991; Kimura et al., 2004; Ward, 1973). Each amphid consists of 12 sensory neurons, possessing specialized receptive endings that respond to distinct cues. These neurons associate with two glial cells, the amphid sheath (AMsh) and amphid socket (AMso) glia, that together form a matrix-filled channel through which sensory cilia of eight neurons are exposed to the external environment (Perkins et al., 1986). The remaining four neurons have elaborately structured receptive endings that are ensheathed by the AMsh glial cell. These glia-ensheathed receptive endings include the branched wing-like cilia of the odor-sensing neurons AWA, AWB, and AWC, as well as the microvilli-like fingers of the AFD thermosensory neuron (Doroquez et al., 2014; Perkins et al., 1986) (Figure 1A).

We previously showed that post-embryonic ablation of AMsh glia, after the amphid had formed, results in defects in the associated sensory neurons (Bacaj et al., 2008). AMsh glia are required for the proper morphology of the AWA, AWC, and AFD sensory neurons and for dye uptake by cilia of channel neurons, which serves to report on neuronal integrity and access to the environment. Glial ablation also results in defects in behaviors mediated by these neurons. However, the molecular mechanisms controlling these interactions were not well understood.

Here, we characterize the molecular basis for the post-embryonic regulation of sensory-neuron morphology and function by AMsh glia. We developed a larval glial cell isolation method using fluorescence-activated cell sorting (FACS), followed by RNA sequencing (RNA-seq), to identify 598 AMsh glia-enriched

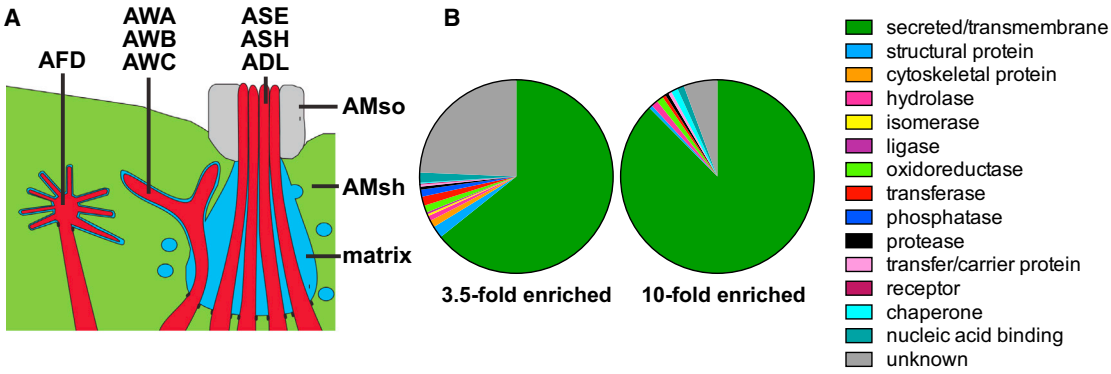


C

| Gene | Wormbase ID | Fold enrichment |
|---|---|---|
| **Known glial genes:** | | |
| *vap-1* | WBGene00006886 | 132 |
| *F11C7.2* | WBGene00017376 | 93 |
| *F53F4.13* | WBGene00009995 | 90 |
| *F16F9.3* | WBGene00017514 | 80 |
| *T02B11.3* | WBGene00020155 | 39 |
| *fig-1* | WBGene00009968 | 35 |
| **New glial genes:** | | |
| *K02E11.4* | WBGene00010513 | 69 |
| *R11D1.3* | WBGene00011244 | 66 |

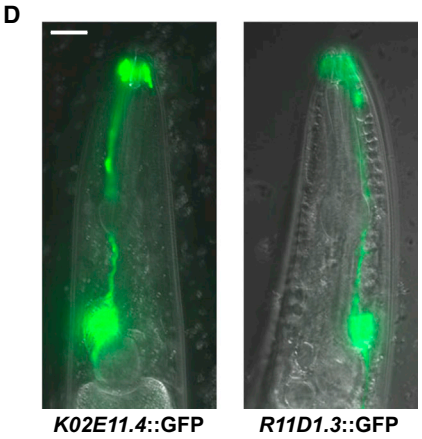


**Figure 1. AMsh Glia-Enriched Genes**

(A) Amphid structure.

(B) AMsh glia transcripts at >3.5-fold or >10-fold over all other cells.

(C) Enrichment levels of known and new genes.

(D) AMsh glia-specific expression of indicated genes. Scale bar represents 10 μm.

See also Table S1.

transcripts. Approximately 90% of highly enriched AMsh genes encode secreted or transmembrane proteins, consistent with a role in regulating neuronal properties. A post-embryonic RNAi screen of a subset of these genes led to the identification of the homeodomain transcription factor *pros-1* as a glial regulator of neuronal morphology and function. Expression studies, cell-specific RNAi experiments, and mosaic rescue experiments confirm that *pros-1* acts in glia to control sensory-neuron shape and function. To characterize the mechanisms mediating *pros-1* functions, we identified *pros-1* target genes using differential gene-expression analyses of AMsh glia isolated from *pros-1* RNAi-treated and control animals. Approximately one-third of AMsh-enriched genes encoding secreted or transmembrane proteins require PROS-1 for their expression, revealing a key function for this gene in regulating expression of the glia-specific secretome. PROS-1 targets include genes with known roles in amphid morphology and function, and the RNAi screens we performed identify new genes that contribute to *pros-1* function. Thus, PROS-1 is a key transcriptional regulator governing the expression of secreted and membrane proteins in AMsh glia.

Prospero, the *Drosophila* homolog of *pros-1*, plays well-known roles in the establishment of cell fate during nervous system development (Doe et al., 1991; Freeman and Doe, 2001). Importantly, we found that while post-embryonic inactivation of *pros-1* by RNAi promotes profound defects in sensory-neuron function, general aspects of glial cell fate are unperturbed, thus revealing functions for this classical cell fate gene in differentiated glia. Prospero homologs are expressed in glia associated with sense organs in many species, including sheath cells in *Drosophila* external sense organs (Manning and Doe, 1999), mechanosensory support cells in fish neuromasts (Pistocchi et al., 2009), and Deiters' cells in the mammalian ear (Bermingham-McDonogh et al., 2006), and are also expressed in astrocytes in *Drosophila* and mammals (Peco et al., 2016) (Zhang et al., 2014). Thus, our studies of *pros-1* function in *C. elegans* provide general insights into the regulation of neuronal function by glia.

## RESULTS

### Identification of Transcripts Enriched in Post-embryonic AMsh Glia

To identify glial genes controlling sensory neuron function, and not development, we isolated AMsh glia from late-stage *C. elegans* larvae and performed gene expression analysis (see

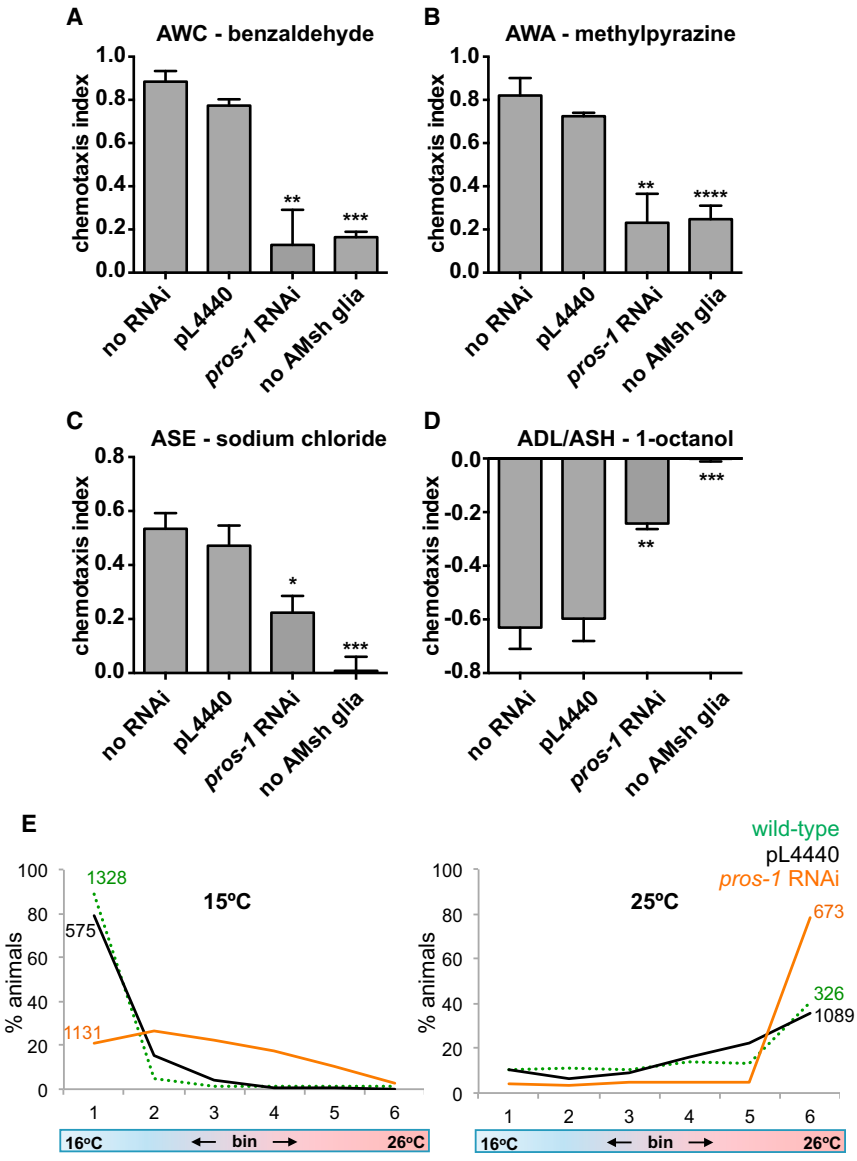


**Figure 2. Post-embryonic *pros-1* RNAi Results in Chemosensory and Thermosensory Defects**

(A–C) Chemotaxis to (A) benzaldehyde, (B) methylpyrazine and (C) sodium chloride. Relevant neurons are indicated above each graph. pL4440, vector control. No AMsh glia, genetic ablation of AMsh glia by expression of diphtheria toxin.

(D) Avoidance of 1-octanol, sensed by ADL and ASH.

(E) *pros-1* RNAi thermotaxis defects. Cultivation temperatures and number of animals scored are indicated.

For (A)–(D) n = 3, mean ± SD. *p = 0.016, **p < 0.01, ***p < 0.001, ****p < 0.0001 (Student's t test).

Experimental Procedures). Cells expressing the AMsh glia-specific reporter *F16F9.3*::dsRed were sorted by FACS and subjected to RNA extraction and purification. mRNA was amplified and used to generate a cDNA library for sequencing. Quantitative gene expression profiling was carried out to identify genes enriched in AMsh glia, by comparing AMsh glia to all other cell types not expressing dsRed. This approach led to the identification of 598 candidate AMsh glia-enriched genes (fold enrichment > 3.5, p-adj < 0.05; see Experimental Procedures for statistical analysis and cutoff rationale). Of these 598 genes, 383 (64%) encode proteins with signal peptides or transmembrane domains (Table S1; Figure 1B). This is significantly higher than the prevalence of such proteins in the *C. elegans* genome (45%) (Suh and Hutter, 2012). Strikingly, of 177 highly enriched AMsh genes (fold enrichment > 10), 155 genes (88%) encode proteins with signal peptides or transmembrane domains (Figure 1B). To validate this gene list, we checked the expression levels of six known AMsh glia-specific genes (Bacaj et al., 2008). All six genes showed strong enrichment in AMsh glia in our analysis (Figure 1C), confirming that we successfully isolated larval AMsh glial transcripts. We also made transcriptional reporters with upstream regulatory regions for two genes, *K02E11.4* and *R11D1.3*, both of which are highly enriched in AMsh glia in our analysis, but not previously studied. Transcriptional reporters for both genes showed specific expression in AMsh glia (Figure 1D), as well as in the analogous phasmid sheath glia in the tail, confirming that we successfully identified AMsh glial genes.

## Glia-Enriched *pros-1*/Prospero Is Required for Sensory-Neuron Function

To uncover the molecular pathways through which AMsh glia regulate functional properties of associated sensory neurons, we screened animals for sensory deficits following post-embryonic RNAi against 140 of the 598 AMsh glia-enriched genes. Following 3 days of RNAi treatment, first-day adults were assessed for defects in chemosensation, using standard chemotaxis and avoidance assays. RNAi targeting mRNAs encoding the Prospero-related transcription factor, PROS-1, results in defects in all chemosensory behaviors tested, including chemotaxis to benzaldehyde, methylpryazine, and sodium chloride, attractants sensed by AWC, AWA, and ASE sensory neurons, respectively. Avoidance of 1-octanol, a repellant sensed by ADL and ASH sensory neurons is also perturbed (Bargmann, 2006; Bargmann et al., 1993; Bargmann and Horvitz, 1991; Chao et al., 2004) (Figures 2A–2D). *pros-1* RNAi animals also exhibit defective thermotaxis behavior (Figure 2E), suggestive of functional defects in the AFD thermosensory neuron. Post-embryonic loss of *pros-1*, therefore, phenocopies ablation of AMsh glia (Bacaj et al.,

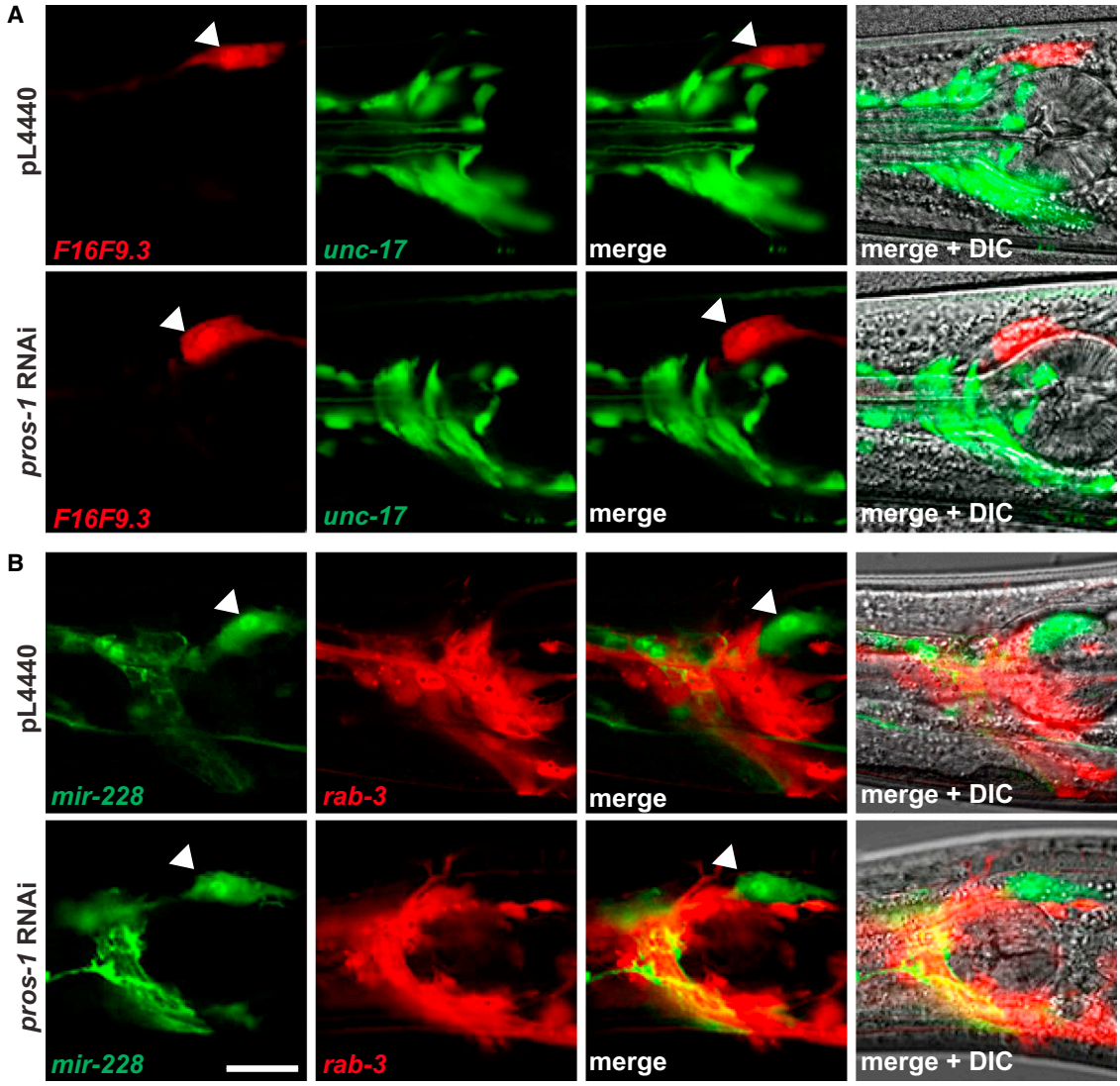


**Figure 3. Post-embryonic *pros-1* RNAi Does Not Affect AMsh Glia Fate**

(A) Animals expressing *F16F9.3*::dsRed, an AMsh glia reporter, and *unc-17*::GFP, a cholinergic neuron reporter.

(B) Animals expressing the pan-glial marker *mir-228*::GFP and the pan-neuronal marker *rab-3*::mCherry. White arrowheads, AMsh glia cell body. Scale bar represents 10 μm.

2008), which also results in functional defects of associated sensory neurons.

## PROS-1/Prospero Functions Post-embryonically and Does Not Affect Glial Cell Fate

In *Drosophila*, Prospero regulates the decision between glial and neuronal fates during external sense-organ formation. Prospero mutants fail to produce glia, and Prospero overexpression results in overproduction of glia and of cells inappropriately expressing both glial and neuronal markers (Manning and Doe, 1999). *C. elegans pros-1* is also expressed in glial cells and their precursors during embryogenesis (expression patterns in *Caenorhabditis* [EPIC], http://epic.gs.washington.edu/); however, we specifically carried out our RNAi studies post-embryonically, after glial and neuronal fate had been established. Thus, the *pros-1*(RNAi) defects we observe may not result from a loss of glial cell fate. Indeed, we found that AMsh glia continue to express glial markers following post-embryonic *pros-1* RNAi, including the AMsh-specific marker *F16F9.3* and the pan-glial marker *mir-228* (Figure 3). Furthermore, *pros-1*(RNAi) AMsh glia do not show inappropriate expression of markers specific to their sister neurons. The cholinergic neuron URB, the sister cell of the AMsh glial cell, expresses *unc-17*/vAChT, a specific marker for cholinergic neurons, as well as *rab-3*, a pan-neuronal marker (Alfonso et al., 1993; Duerr et al., 2008). Neither is expressed in AMsh glia of *pros-1*(RNAi) animals, nor are AMsh reporters expressed in URB (Figure 3). Finally, AMsh glia of *pros-1*(RNAi) animals are grossly normal in morphology

(see below). These results indicate that the defects we observed following *pros-1* RNAi are not a result of general cell-fate abnormalities. Thus, *pros-1* controls specific post-developmental aspects of glial function.

## Animals Lacking PROS-1/Prospero Exhibit Defects in Sensory Neuron Receptive-Ending Structure and Microenvironment

To uncover the cellular basis for the behavioral deficits exhibited by *pros-1*(RNAi) animals, we assessed the morphology of sensory-neuron receptive endings and the structure of the AMsh glial membranes surrounding these receptive endings using fluorescence and electron microscopy. The AWC odor-sensing neuron and the AFD thermosensory neuron both have elaborate receptive endings that are ensheathed by AMsh glia (Figure 1A). Following *pros-1* RNAi, both neurons extend dendrites normally to the tip of the nose, but their receptive endings are largely absent. AWC neurons lack the wing-like cilium found in wild-type adults (Figures 4A and 4F), while AFD neurons lack the microvilli-like fingers found in wild-type adults (Figures 4B, 4C, and 4F).

In contrast to neurons with glia-ensheathed receptive endings, the ASE channel neuron does not show morphological defects following *pros-1* RNAi, with an apparently normal cilium at the tip of the dendrite (Figures 4D and 4F). However, unlike wild-type animals, ASE and other channel neuron cilia are not exposed to the environment following *pros-1* RNAi treatment. While the overall morphology of the AMsh glial cell appears normal when assessed by fluorescence microscopy (Figures 4E and 4F), electron microscopy reveals striking defects in the glial channel housing sensory-neuron receptive endings (Figure 4G). In wild-type animals, neurons with simple cilia penetrate through the AMsh glial cell and enter an extracellular channel, generated by these glia. This channel is filled with an electron-dense extracellular matrix, secreted by AMsh glia, and is thought to be important for sensory function (Perkins et al., 1986) (Bacaj et al., 2008). The channel formed by the AMsh glial cell is continuous with an opening through the cuticle formed by the anteriorly positioned AMso glial cell (Figures 1A and 4G). Animals treated with *pros-1* RNAi show a striking defect in amphid channel architecture. At the posterior position, where cilia normally enter the glial channel, individual cilia of *pros-1*(RNAi) animals are surrounded by the AMsh cell, but the channel is indistinct and glia-secreted matrix material is absent (Figure 4G, bottom). More anteriorly, cilia that normally access the environment are blocked by an electron-dense deposit (Figure 4G, top). To confirm these structural defects, we assessed the accessibility of channel-neuron cilia to the environment by carrying out dye-filling assays. In wild-type animals, a subset of exposed channel neurons can take up dye. Consistent with the channel defects we observed by electron microscopy, *pros-1*(RNAi) animals are unable to take up dye (Figure 4H).

In summary, *pros-1* is required post-embryonically for maintenance of the glial channel through which channel neurons are normally exposed to the environment, for secretion of the extracellular matrix surrounding channel neurons, and for the proper morphology of the receptive endings of other glia-ensheathed neurons. Defects in these functions are consistent with the behavioral deficits we observed in *pros-1*(RNAi) animals and suggest a role for *pros-1* in regulating aspects of glial membrane structure and secretion.

## PROS-1/Prospero Functions in Glia to Control Neuron Structure and Function

We identified *pros-1* as a candidate glial regulator of neuronal function based on AMsh glia expression profiling. To confirm that *pros-1* expression is indeed prominent in these glia, we examined animals carrying a recombineered fosmid expressing a C-terminally tagged PROS-1::GFP reporter under the control of *pros-1* genomic regulatory elements. PROS-1::GFP is detected in the nuclei of AMsh glia (Figure 5A), confirming our expression profiling data. Importantly, PROS-1::GFP is not detected in amphid sensory neurons, identified by specific markers for AWC and AFD glia-ensheathed neurons and by DiI-staining for channel neurons (Figures 5B–5D). PROS-1::GFP is also not detected in the AMso glia (Figure 5E). PROS-1::GFP is detected in many other sense organ-associated glia in the head, including the astrocyte-like CEP sheath glia, and the glia of the inner and outer labial sensilla (Figure S1), suggesting that *pros-1* may play conserved roles in regulating sensory function across sense organs.

The expression of *pros-1* in AMsh glia, but not in amphid sensory neurons, is consistent with the hypothesis that *pros-1* functions within glia, controlling glial channel morphology and extracellular matrix secretion cell autonomously and sensory-neuron receptive-ending shapes and functions through a non-cell-autonomous mechanism. To test this idea, we used two approaches. First, we generated a transgenic strain for glia-specific RNAi by restoring expression of the Argonaute protein RDE-1 specifically in AMsh glia in an *rde-1(ne219)* mutant background. *rde-1* is essential for RNAi induced by exogenous double-stranded RNA (dsRNA) and is required for incorporation of processed small interfering RNAs (siRNAs) into silencing complexes but is not required for the intercellular transport of dsRNA precursors (Parrish and Fire, 2001; Tabara et al., 1999). *rde-1(ne219)* mutant animals therefore take up dsRNA but cannot carry out RNAi. Expression of *rde-1* under an AMsh glia-specific promoter thus results in AMsh glia-specific gene silencing after dsRNA feeding. Importantly, AMsh glia-specific *pros-1* RNAi results in the same defects observed using systemic *pros-1* RNAi, including amphid channel neuron dye-filling, sodium chloride chemotaxis, and benzaldehyde chemotaxis defects (Figures 5F–5H), albeit with reduced penetrance. This can be explained, at least in part, by our finding that AMsh glia RNAi efficiency is reduced in this transgenic strain (S.W.W. and S.S., unpublished data).

## A Genetic Lesion in *pros-1* Resembles *pros-1*(RNAi)

To further confirm that *pros-1* expression is required in AMsh glia for sensory neuron function, we characterized a *pros-1* deletion mutant, *tm258*, provided by the NBP (National Biosciences Project) as a *pros-1(tm258)*/hT2 balanced strain. *tm258* is a large deletion and is predicted to be a null allele. *pros-1(tm258)* mutant animals show greatly reduced larval viability, characterized by slow larval development and larval lethality. On rare occasions, *pros-1(tm258)* mutants survive to adulthood but usually fail to

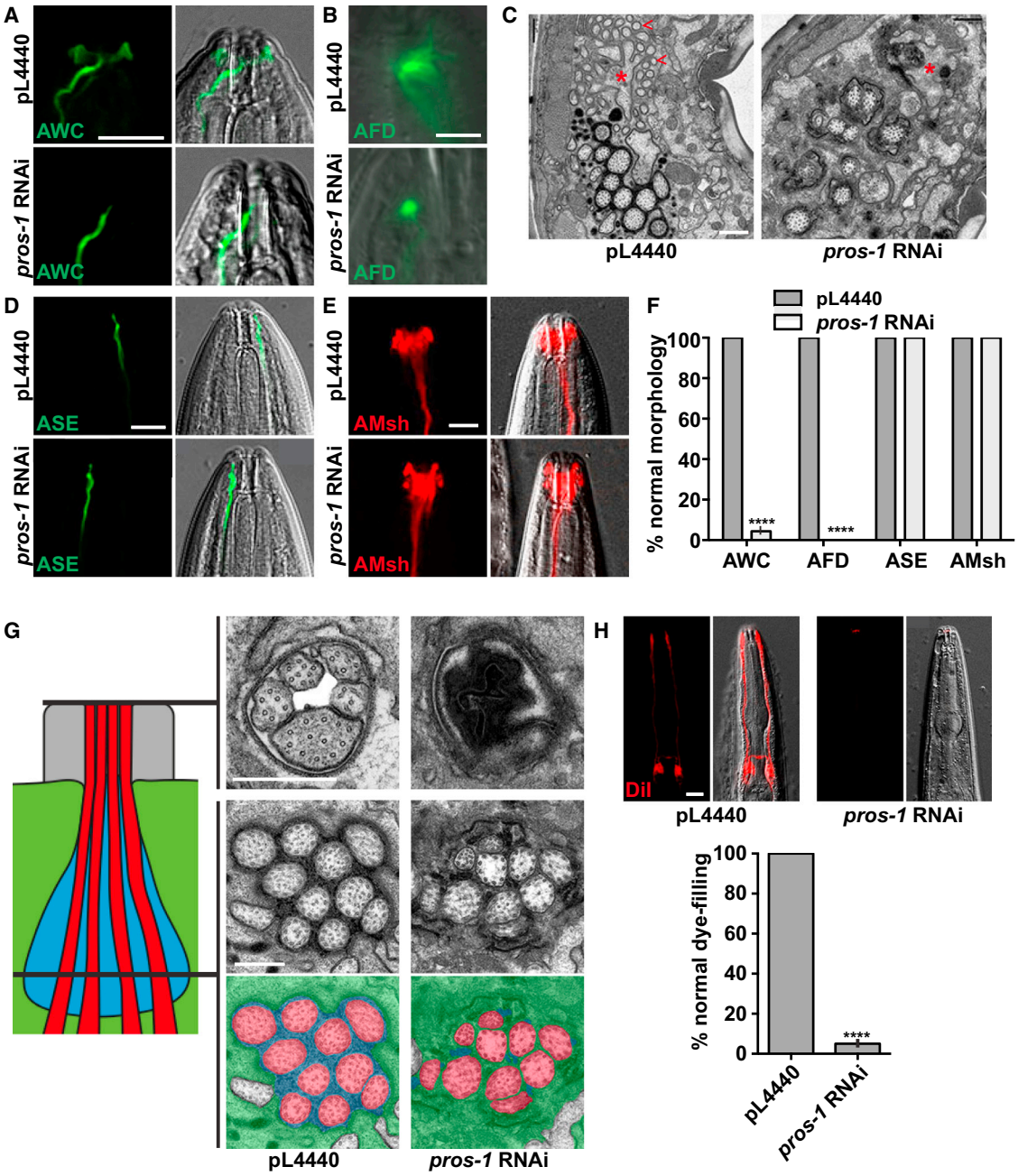


**Figure 4. *pros-1* Regulates the Morphology of Glia-Ensheathed Neuronal Receptive Endings and the Amphid Channel Structure**

Scale bar represents 10 μm, unless stated otherwise.

(A) AWC neuronal receptive endings (NREs), visualized with *odr-1*::YFP.

(B) AFD NREs, visualized with *srtx-1*::GFP. Scale bar represents 5 μm.

(C) Electron micrographs confirm loss of AFD microvilli after *pros-1* RNAi (asterisk, AFD dendrite; arrowheads, AFD microvilli). Scale bar represents 0.5 μm.

(D) ASE NREs, visualized with *gcy-5*::GFP.

(E) AMsh glia, visualized with *F16F9.3*::dsRed.

(F) Quantification of morphologies assessed by fluorescence microscopy in (A) (lack of wing-like cilium), (B) (lack of microvilli-like fingers), (D) (normal channel cilium), and (E) (normal sheath membrane). Error bars represent SEM. AWC n > 100, AFD n > 70, ASE n > 20, and AMsh n > 50; ****p < 0.0001 (z test).

(G) Left: amphid channel schematic (green, AMsh glia; red, channel neuron cilia; blue, glial-secreted extracellular matrix; gray, AMso glia). Right: corresponding electron micrographs at two sections through the amphid. Scale bar represents 0.5 μm.

(H) Top: *pros-1* RNAi amphid neuron dye-filling defect. Bottom: quantification of dye-filling defect. Error bars represent SEM, n = 150; ****p < 0.0001 (z test).

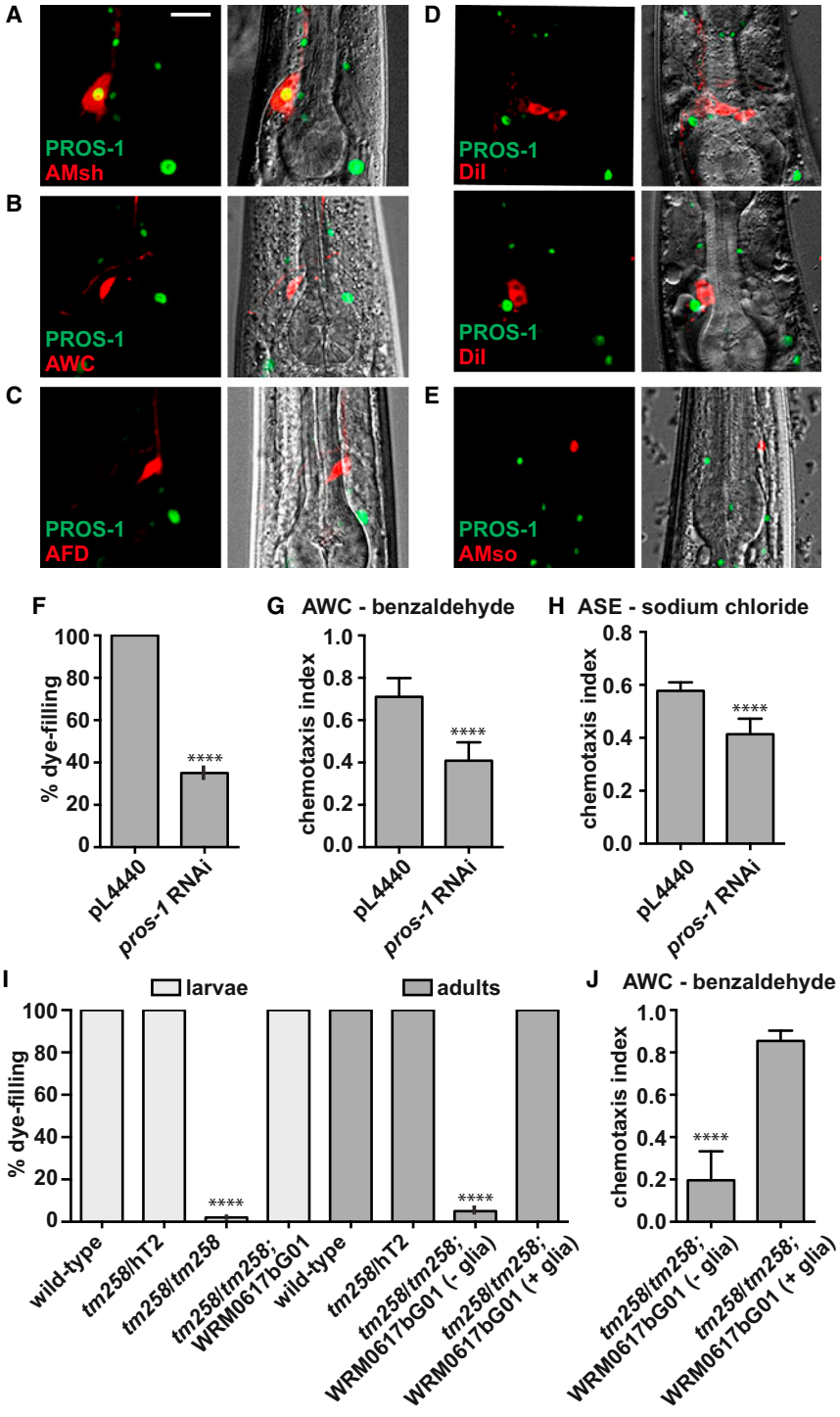


**Figure 5. *pros-1* Is Expressed and Functions in AMsh Glia to Regulate Neuronal Properties**

(A–E) PROS-1::GFP translational reporter under the control of *pros-1* genomic elements. Scale bar represents 10 μm. (A–C and E) AMsh glia, AWC, AFD, and AMso marked with *F16F9.3*::dsRed, *odr-1*::RFP, *srtx-1*::mCherry, or *itr-1*::NLS-RFP, respectively. (D) Amphid channel neurons, identified by DiI staining. Two sections from the same animal are shown.

(F–H) AMsh glia-specific RNAi using *rde-1(ne219)* RNAi deficient strain expressing *rde-1* in AMsh glia. (F) Amphid neuron dye filling; n > 200, error bar represents SEM; ****p < 0.0001 (z test). (G and H) Benzaldehyde and sodium chloride chemotaxis; n = 7, mean ± SD; ****p < 0.0001 (Student's t test).

(I and J) *pros-1(tm258)* deletion mutant. (I) Dye-filling defects of indicated genotypes. WRM0617bG01, fosmid covering *pros-1* locus. +/− glia, fosmid present/absent in AMsh glia. Error bar represents SEM; larvae n = 300, adults n > 200; ****p < 0.0001 (z test). (J) Same as (I) but showing the benzaldehyde chemotaxis assay. n = 5, mean ± SD; ****p < 0.0001 (Student's t test).

See also Figure S1.

give progeny. *pros-1(tm258)* larvae show highly penetrant amphid neuron dye-filling defects (Figure 5I). Larval viability and dye-filling defects are not seen in *pros-1(tm258)*/hT2 heterozygotes, indicating that a single copy of *pros-1* is sufficient for *pros-1* function. Larval viability and amphid neuron dye-filling defects in *pros-1(tm258)* mutants can be rescued with a fosmid covering the *pros-1* locus, indicating that these defects are a specific consequence of *pros-1* loss (Figure 5I).

The larval growth defects precluded direct analysis of *pros-1(tm258)* adults. To overcome this, we took advantage of the mosaic expression pattern of extrachromosomal arrays and analyzed *pros-1(tm258)* adults that contain a rescuing *pros-1* fosmid as an unstable array but lack expression of the array in AMsh glia, based on a glia-specific GFP co-injection marker. Such mosaic transgenic *pros-1(tm258)* animals showed normal larval development, indicating that the larval-development defects are not a result of *pros-1* loss in AMsh glia. Importantly, mosaic adults lacking *pros-1* expression in AMsh glia showed the same amphid neuron dye-filling defects and benzaldehyde chemotaxis defects observed following *pros-1* RNAi, while control animals with the *pros-1* rescuing fosmid present in AMsh glia showed normal responses (Figures 5I and 5J). These results confirm the specificity of the RNAi phenotype observed and support our conclusion that *pros-1* expression is required in AMsh glia for sensory function.

## Many PROS-1 Target Genes Encode Secreted Proteins

*pros-1* encodes a homeodomain transcription factor. To identify target genes that mediate *pros-1* activity, we first looked at

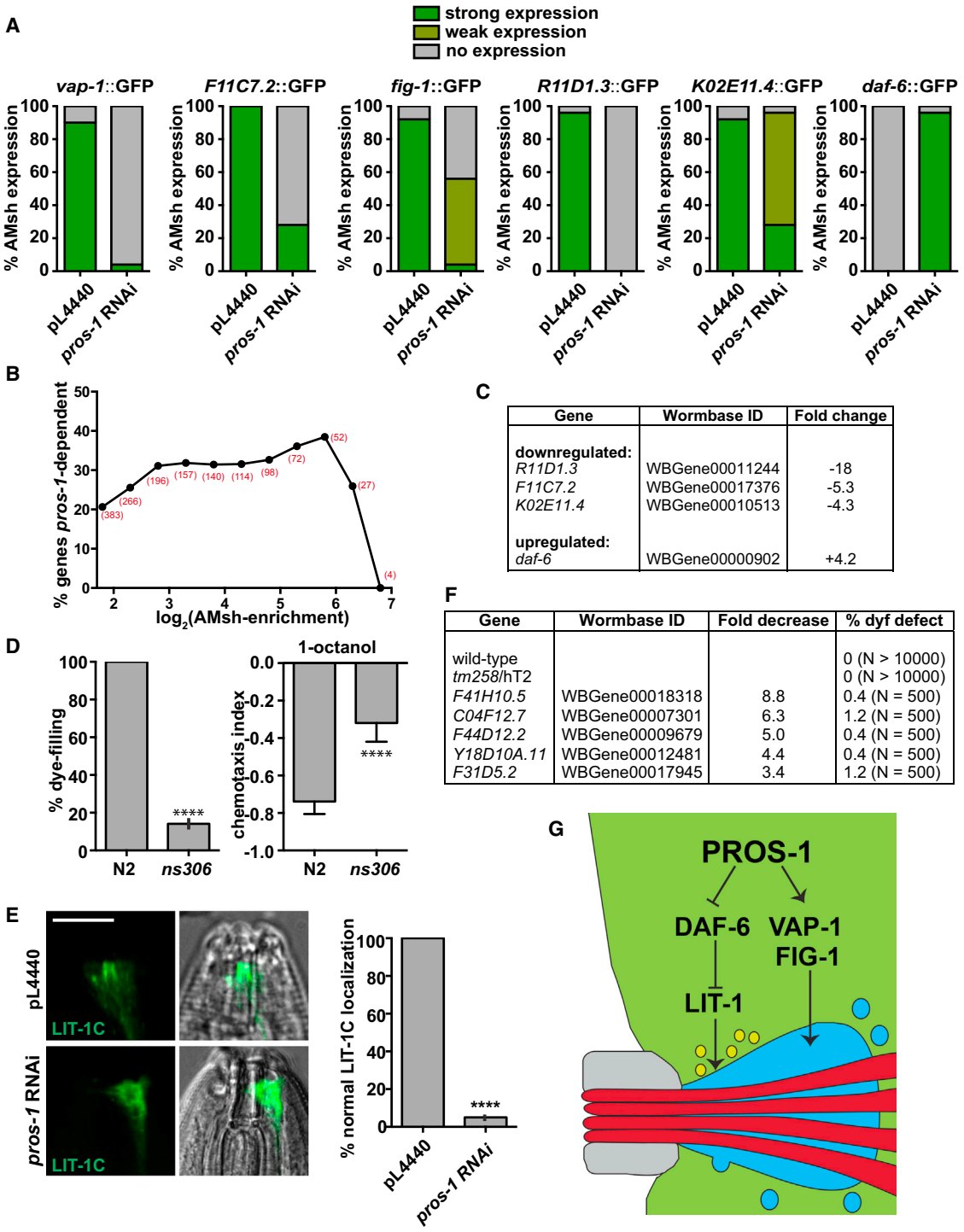


**Figure 6. *pros-1* Target Genes in AMsh Glia**

(A) AMsh glia-specific gene expression with *pros-1* RNAi.

(B) AMsh glia secreted/transmembrane gene enrichment correlates with *pros-1*-dependency. Genes with indicated value or higher enrichment are scored for being PROS-1 targets. Red numbers indicate the number of genes in each data point. For very high glial enrichment levels, gene numbers are low.

(C) *pros-1*-dependent genes discussed in the text.

(D) *fig-1(ns306)* dye-filling defects (error bars represent SEM, n > 80; ****p < 0.0001, z test) and 1-octanol avoidance defects (n = 5, mean ± SD; ****p < 0.0001, Student's t test).

(E) LIT-1C localization in AMsh glia. Scale bar represents 10 μm. Right: error bar represents SEM, n > 300; ****p < 0.0001 (z test).

*(legend continued on next page)*

expression of known AMsh glia genes. Animals treated with *pros-1* RNAi showed a strong reduction in expression of the glial genes *vap-1*, *F11C7.2*, and *fig-1*, as determined by analysis of transcriptional reporters (Figure 6A). *vap-1* encodes a secreted protein with conserved cysteine-rich secretory protein, antigen 5, and pathogenesis-related 1 (CAP) domains, found in cysteine-rich secretory proteins that play a role in regulating extracellular matrix remodeling, whereas *F11C7.2* and *fig-1* encode secreted proteins containing conserved TSP-1 (thrombospondin type 1) domains, found in extracellular matrix proteins including thrombospondins, known to be involved in glia-neuron interactions (Christopherson et al., 2005; Gibbs et al., 2008).

To identify additional *pros-1*-dependent genes, we isolated AMsh glia using FACS and carried out gene expression profiling from *pros-1* RNAi-treated and control animals. Cells were isolated from late-stage larvae (L3 and L4) grown postembryonically for 36–42 hr in liquid cultures of *E. coli* HT115 for RNAi by feeding. This time point was chosen because time-course experiments showed that *pros-1*(RNAi) defects of animals treated from the first larval stage (L1) become apparent at L3/4 (Figure S2), most likely enriching for primary transcriptional targets. Effectiveness of RNAi by feeding when animals are grown in liquid culture was verified with dye-filing assays (Figure S2).

Homeodomain transcription factors, including the *pros-1* homolog Prospero, can act as both positive and negative regulators of transcription (Choksi et al., 2006), and, indeed, we found glial genes with either decreased or increased expression levels following *pros-1* RNAi. 439 genes show a significant reduction in expression (Table S2), while 634 genes show a significant increase (Table S3; see Experimental Procedures for statistical analysis). Comparison of AMsh-enriched genes encoding secreted or transmembrane proteins with *pros-1*-dependent genes revealed a positive correlation between the degree of enrichment in AMsh glia and likelihood of being a *pros-1* target (Figure 6B). Strikingly, of the 155 highly enriched (>10×) AMsh glia genes that encode proteins with signal peptides or transmembrane domains (Figure 1), 49 genes (32%) showed a significant reduction in expression following *pros-1* RNAi. Thus, *pros-1* controls the expression of a large portion of the AMsh glia-specific secretome (along with other genes; Figure S3), consistent with the defects in extracellular matrix secretion and membrane abnormalities we observed in *pros-1* mutants.

To validate the candidate *pros-1* target genes we identified, we assessed the expression levels of transcriptional reporters for two genes, *R11D1.3*, encoding a secreted protein of unknown function, and *K02E11.4*, encoding a secreted protein containing a conserved uridine 5′-diphosphate (UDP)-glucoronosyltransferase domain, found in enzymes that act in the olfactory epithelium to modulate chemosensory cues (Leclerc et al., 2002). These were identified in our RNA-seq studies as having 18-fold and 4.3-fold decreased expression in *pros-1* RNAi animals (Figure 6C). Importantly, both reporters show clear reductions in AMsh glia GFP expression in animals treated with *pros-1* RNAi (Figure 6A). The reduction in expression is particularly strong for *R11D1.3*::GFP, which correlates with the increased *pros-1* dependence of this gene seen in our expression profiling data. These results confirm that we identified *pros-1*-dependent genes in our expression profiling experiments.

Of the genes we identified as *pros-1* dependent based on transcriptional reporters (*vap-1*, *fig-1*, and *F11C7.2*; Figure 6A), only *F11C7.2* also showed *pros-1* dependence in our expression profiling (Figure 6C). One explanation for this difference may be in the timing of the experiments. Reduction in transcriptional reporter expression was observed in adults after 3 days of RNAi treatment, while we isolated AMsh glia from late-stage larvae at 36–42 hr of RNAi treatment. Thus, *fig-1* and *vap-1* may represent secondary targets for PROS-1.

Taken together, our expression profiling studies, coupled with phenotypic analysis of *pros-1* mutants, reveal that PROS-1 is a major regulator of the AMsh glia secretome.

## PROS-1 Target Genes Encoding Membrane and Secreted Proteins Account for Neuronal Dye-Filling Defects in *pros-1* Mutants

To identify functionally important genes whose expression changes contribute to the defects observed in *pros-1* mutants, we searched for known regulators of AMsh glial function among our list of candidate *pros-1*-dependent genes and carried out additional RNAi screens.

As described above, expression of the *fig-1* gene is strongly dependent on *pros-1*. *fig-1* encodes a secreted thrombospondin-domain-containing extracellular matrix protein necessary for amphid neuron dye-filling and avoidance of 1-octanol (Figure 6D) (Bacaj et al., 2008). Thus, *pros-1* acts in glia to control neuronal function and to regulate the amphid channel extracellular microenvironment partly by promoting expression of FIG-1 protein.

We also found that expression of the Patched-related gene *daf-6*, a negative regulator of amphid channel expansion, increases significantly following *pros-1* RNAi (4.2-fold increase), a result we confirmed by analysis of a *daf-6*::GFP expression reporter (Figure 6A). DAF-6 is a membrane protein that restricts amphid channel size, and *daf-6* mutants have abnormally expanded channels. Thus, overexpression of DAF-6 may contribute to the loss of amphid channel membrane following *pros-1* RNAi. Supporting these observations, DAF-6 functions by antagonizing the activity of *lit-1*, a Nemo-like kinase that localizes to the amphid channel membrane and promotes channel expansion (Oikonomou et al., 2011). Although *lit-1* expression level was not affected in *pros-1*(RNAi) animals, LIT-1 protein, which normally lines the amphid channel, showed only diffuse localization (Figure 6E). Together, these results suggest that *pros-1* acts, at least in part, to regulate amphid channel size by inhibiting expression of *daf-6* to support *lit-1* function.

(F) *pros-1*-dependent genes have dye-filling defects ($p < 0.0001$ z test).
(G) Model for PROS-1 function in controlling glial membrane structure and secretion. DAF-6 and LIT-1 control channel size, and VAP-1 and FIG-1 are extracellular matrix components.
See also Figures S2 and S3 and Tables S2 and S3.

Finally, to identify additional genes mediating *pros-1* function, we screened candidate *pros-1* target genes by RNAi for defects in amphid neuron dye filling. To compensate for possible redundancy among *pros-1* target genes, we carried out these experiments in *pros-1(tm258)*/hT2 heterozygous animals, which show normal dye filling (Figure 5I) but which we predict to have reduced levels of *pros-1* expression and may in turn have reduced expression of redundantly acting target genes and therefore provide a sensitized background for detecting functional defects. Indeed, *pros-1(tm258)*/hT2 heterozygotes treated with RNAi against the gene *rdy-2*, previously identified as required for dye filling (Liégeois et al., 2007), show increased defects compared to *rdy-2*(RNAi) animals alone (56% defective versus 16%). This screen identified five candidate *pros-1* target genes that exhibit low, but statistically significant, dye-filling defects and thus may represent functional targets of *pros-1* in AMsh glia (Figure 6F). Notably, all are predicted to encode proteins with transmembrane domains.

## DISCUSSION

### Differences between Embryonic and Post-embryonic Glial Transcriptomes

The amphid sense organ of *C. elegans* is an attractive model system for studying interactions between glia and neurons because of its relatively simple anatomy and because the functional properties of amphid sensory neurons have been extensively studied (Shaham, 2006, 2015). To characterize the molecular mechanisms through which AMsh glia regulate neuronal function, and not development, we took advantage of recently developed larval cell isolation techniques and adapted these to identify AMsh glia post-embryonic transcripts by RNA-seq (Spencer et al., 2014; Zhang and Kuhn, 2013). This approach led to the identification of 598 candidate AMsh glial genes. We previously identified 298 transcripts enriched in embryonic AMsh glia (Bacaj et al., 2008). Of the 598 post-embryonic transcripts identified in this study, only 72 were also detected in our previous study. While the large number of newly identified transcripts can be partly explained by differences in transcript analysis and statistical methods used (RNA-seq versus microarray), this difference highlights the advantage of using larval cell isolation for identification of genes with post-embryonic functions and reveals distinct transcriptomes for these stages.

### PROS-1 Is a Regulator of the Glial Secretome

Here, we demonstrate that RNAi against *pros-1* results in similar defects to AMsh glia ablation, including defective morphology of glia-ensheathed sensory-neuron receptive endings and defective functions of channel neurons. *pros-1* was previously noted to affect larval survival and amphid neuron dye filling (Kolotuev et al., 2013), and its role in excretory canal formation was characterized in detail, but the nature of the amphid neuron dye-filling defect was not previously explored. Importantly, in this study, we show that *pros-1* is expressed in AMsh glia, as well as glia of other sense organs, but not in amphid neurons, and is required for maintenance of the matrix-filled amphid channel, through which channel neurons are exposed to the external environment, and for sensory behaviors controlled by these neurons. Additionally, we have shown that *pros-1* is required for proper morphology of the glia-ensheathed receptive endings of odor- and thermosensory neurons and that *pros-1* loss of function results in defects in the corresponding chemotaxis and thermotaxis behaviors. *pros-1* thus acts cell autonomously to maintain amphid channel structure and non-cell autonomously to maintain the receptive endings of ensheathed sensory neurons, perhaps through glia-to-neuron signaling. Both glia-neuron communication and amphid channel shape and content are predicted to require secreted and/or transmembrane proteins. Consistent with this idea, AMsh glia show a striking over-representation of genes encoding secreted or transmembrane proteins, of which approximately one-third are *pros-1* dependent. PROS-1 is, therefore, a key regulator of the AMsh glia secretome. Of note, our expression profiling experiments also reveal that *pros-1* regulates expression of non-secreted genes, suggesting *pros-1* has additional functions.

Some *pros-1* targets we identified, such as *fig-1* and *daf-6*, may partly explain the defects we observe in *pros-1* mutants (Figure 6G), as these components have known independent roles in AMsh glia. The large number of *pros-1* target genes we identified suggests that other targets may act redundantly, making the identification of functionally important target genes challenging. Remarkably, the robustness of amphid neuron dye filling in wild-type animals allowed us to identify weak but statistically significant defects in five candidate *pros-1* target genes. Of these, *F41H10.5* encodes a transmembrane protein with a conserved TLC (TRAM, LAG1, and CLN8) domain, which have general roles in lipid metabolism and in mammals regulate calcium channel activity (Papanayotou et al., 2013; Winter and Ponting, 2002), and *F31D5.2* encodes a transmembrane protein with a major facilitator superfamily domain, a conserved domain found in solute transporters (Yan, 2015). While the remaining three genes encode proteins of unknown function, it is notable that all three encode predicted transmembrane proteins. While further work is required to assess the roles of these genes in *pros-1*-mediated functions, these observations are consistent with roles in glia-neuron interactions.

### PROS-1/Prospero Has Cell-Fate-Independent Functions

*pros-1* encodes a Prospero-related homeodomain transcription factor. Prospero has well-known roles in determining cell-fate decisions during nervous system development in *Drosophila* (Doe et al., 1991). When neuroblasts divide, Prospero is distributed asymmetrically between daughter cells and promotes differentiation of ganglion mother cells into neurons and glia by inhibiting expression of cell-cycle genes and promoting expression of genes for terminal differentiation (Choksi et al., 2006; Freeman and Doe, 2001). During the final round of cell divisions generating external sense organs in *Drosophila*, a precursor cell divides to produce a glia-like sheath cell and a neuron. Prospero mutants produce neither, while Prospero overexpression results in overproduction of glia and causes a partial neuron-to-glia fate conversion (Manning and Doe, 1999). Prospero expression is downregulated in neurons after the final cell division but is retained in glia. Notably, in Prospero mutants that do generate neurons, these exhibit defective axon and dendrite morphology. Although this defect might reflect a role

for the transient expression of Prospero in neurons, our results raise the possibility that the defects may originate from the glia-like sheath cell.

In addition to sheath cells in the sense organs of the *Drosophila* wing, Prospero is also expressed in the glia-like support cells of the antenna-maxillary complex (AMC), the larval chemosensory organ (Balakireva et al., 2000). Expression profiling to identify Prospero-dependent genes in whole-AMC extracts was performed (Guenin et al., 2010). However, Prospero is expressed in neurons and glia-like cells of the AMC, and reported targets are mainly involved in neuronal axon growth and synaptic function and therefore likely to represent Prospero targets in neurons and not support cells.

Vertebrate homologs of Prospero are expressed throughout the nervous system. In the mammalian brain, Prox1 is expressed in the hippocampus, is involved in neurogenesis, and likely has a role in establishing cell fate (Galeeva et al., 2007; Elsir et al., 2012). Prox1 is also expressed in differentiated glia-like support cells in sense organs, including support cells of the mammalian cochlea and the zebrafish neuromast (Bermingham-McDonogh et al., 2006; Pistocchi et al., 2009). Prox1 is expressed in progenitor cells during cochlea development, but post-embryonically, its expression is restricted to glia-like cells, including Deiters' cells and pillar cells (Bermingham-McDonogh et al., 2006). Prox1 loss in neuromast support cells results in defective uptake of dye by associated mechanosensory hair cells, suggestive of functional defects (Pistocchi et al., 2009). These observations show that expression of Prospero homologs is a conserved feature of sense-organ-associated glia. Importantly, our results suggest that Prospero is likely to be a key factor maintaining the functions of these organs well past embryonic development.

## EXPERIMENTAL PROCEDURES

### Strains and Plasmids

*C. elegans* strains were maintained using standard methods (Stiernagle, 2006). Wild-type strain is Bristol N2. See the Supplemental Experimental Procedures for details of alleles and transgenic strains.

### RNAi

Standard RNAi was carried out as described previously (Kamath and Ahringer, 2003). Overnight cultures of *E. coli* HT115 carrying pL4440 expression vectors targeting specific genes (Ahringer Library and Vidal Library) were seeded on to nematode growth medium plates supplemented with carbenicillin (25 μg/ml) and isopropyl β–D-1-thiogalactopyranoside (1 mM). After 1–2 days of induction at room temperature, embryos obtained from bleaching gravid adults were added to the RNAi plates. Unless stated otherwise, animals were scored 3 days later, as first-day adults.

### Behavioral Assays

All behavior assays were performed on first-day adults. Chemotaxis assays, avoidance assays, and thermotaxis assays were carried out using standard procedures (Bargmann et al., 1993; Chao et al., 2004; Ryu and Samuel, 2002; Ward, 1973). See the Supplemental Experimental Procedures for details. Statistical analysis was performed with an unpaired Student's t test (GraphPad).

### Dye-Filling Assays

DiI (1,1′-dioctadecyl-3,3,3′3′-tetramethylindocarbocyanine perchlorate) (Sigma) stock solution was made at 5 mg/ml in N,N-dimethylformamide. Animals were stained with DiI (stock solution diluted 1:1000 in M9 buffer) for 30–60 min, followed by three M9 washes to remove excess dye. Dye filling was scored as % animals that show amphid neuron dye uptake, with statistical analysis performed with a two-proportion z test (in silico).

### Fluorescence and Electron Microscopy

Fluorescence and electron micrographs were obtained using standard procedures. See the Supplemental Experimental Procedures for details. Quantification of morphological defects assessed by fluorescence microscopy was carried out by scoring individual animals for wild-type versus defective morphology, with statistical analysis performed with a two-proportion z test (in silico).

### Cell Isolation and FACS Analysis

Briefly, synchronized larvae were grown from L1 in liquid culture of *E. coli* HT115 for RNAi treatment. After growth for 36–42 hr, cells were isolated from late-stage larvae (L3 and L4) by protease treatment and mechanical disruption, as described previously (Zhang and Kuhn, 2013), with modifications (Menachem Katz, personal communications). AMsh glia expressing a dsRed transgene (*nsIs143*) were sorted using a BD FACS Aria sorter (Rockefeller University Flow Cytometry Resource Center). See the Supplemental Experimental Procedures for details.

### RNA Isolation and Sequencing

RNA was extracted from TRIzol LS (Ambion)-treated cells by phase separation, following the manufacturer's guidelines. RNA was purified using PicoPure RNA isolation kit (Arcturus). 1–5 ng purified total RNA was obtained per sample. All subsequent steps were performed by the Rockefeller University Genomics Resource Center. RNA quality was verified to make sure sample degradation had not occurred (Agilent Bioanalyzer). mRNA amplification and cDNA preparation were performed using the SMARTer mRNA amplification kit (Clontech). Labeled samples were sequenced using an Illumina HiSeq 2000 sequencer.

### RNA-Seq Quality Assessment and Differential Gene Expression Analysis

Sequence quality was assessed and gene alignment was carried out as described in the Supplemental Experimental Procedures. Three independent replicates were obtained from control animals, and four independent replicates were obtained for *pros-1* RNAi animals. Two different statistical methods were used for differential gene expression analysis, DESeq and voom. For DEseq analysis, DESeq2 was applied to normalize count matrix and to perform differential gene expression on the counts using negative binomial distribution (Love et al., 2014); for voom analysis, edgeR (Robinson et al., 2010) was applied to normalize count matrix, and voom (Law et al., 2014) was applied for gene differentiation analysis. Significant genes from both analyses were combined.

To identify transcripts enriched in AMsh glia compared to other cells (control AMsh versus control non-AMsh), we used a fold change of 3.5 and an adjusted p value threshold of $<0.05$. This fold change cutoff was determined as follows. We sought genes that are >4-fold enriched in AMsh glia, as these changes can be easily assayed in vivo using GFP reporters. For genes showing pan-glial expression, a true enrichment of R should correspond to an RNA-seq-detected enrichment of $959/(46+(909/R))$, assuming each animal has 959 total cells and 50 glial cells. For $R = 4$, RNA-seq enrichment is 3.5×. To identify genes whose expression is regulated by *pros-1* (*pros-1* RNAi AMsh versus control AMsh), we used a less stringent threshold to take into account possible variation in RNAi efficiency between replicates (fold change > 2, adjusted p value $< 0.1$). To identify putative secreted or transmembrane genes, we used Phobius, a combined membrane topology and signal peptide predictor (Stockholm Bioinformatics Center; http://phobius.sbc.su.se).

## ACCESSION NUMBERS

The accession number for the RNA-seq data generated in this study is ENA: PRJEB12954.

## SUPPLEMENTAL INFORMATION

Supplemental Information includes Supplemental Experimental Procedures, three figures, and three tables and can be found with this article online at http://dx.doi.org/10.1016/j.celrep.2016.03.051.

## AUTHOR CONTRIBUTIONS

S.W.W. and S.S. conceived of the studies, designed experiments, interpreted data, and wrote the paper. A.S. performed the studies on AFD neuron (thermotaxis and morphology). Y. Liang performed most of the RNA-seq analysis. Y. Lu performed the electron microscopy studies. S.W.W. performed all the other studies.

## ACKNOWLEDGMENTS

We thank Menachem Katz for help with cell isolation and gene expression analysis, Anupriya Singhal for help with data analysis, and S.S. lab members for helpful discussions. We thank the Rockefeller University Bio-Imaging, Flow Cytometry, and Genomics Resource Centers for outstanding technical support. S.W.W. was a William N. and Bernice E. Bumpus Foundation postdoctoral fellow. A.S. was an American Cancer Society postdoctoral fellow (PF1308301DDC), an NIH-T32 postdoctoral fellow (5T32CA967334), and a Murray Foundation fellow. Y. Liang is supported by the NIH Center for Clinical and Translational Science Award (CTSA) and National Center for Advancing Sciences (NCATS). This work was supported in part by NIH grant R01NS064273 to S.S.

Received: January 28, 2016
Revised: February 25, 2016
Accepted: March 12, 2016
Published: April 7, 2016

## REFERENCES

Alfonso, A., Grundahl, K., Duerr, J.S., Han, H.P., and Rand, J.B. (1993). The Caenorhabditis elegans unc-17 gene: a putative vesicular acetylcholine transporter. Science *261*, 617–619.

Bacaj, T., Tevlin, M., Lu, Y., and Shaham, S. (2008). Glia are essential for sensory organ function in C. elegans. Science *322*, 744–747.

Balakireva, M., Gendre, N., Stocker, R.F., and Ferveur, J.F. (2000). The genetic variant Voila causes gustatory defects during Drosophila development. J. Neurosci. *20*, 3425–3433.

Bargmann, C.I. (2006). Chemosensation in C. elegans. WormBook, 1–29.

Bargmann, C.I., and Horvitz, H.R. (1991). Chemosensory neurons with overlapping functions direct chemotaxis to multiple chemicals in C. elegans. Neuron *7*, 729–742.

Bargmann, C.I., Hartwieg, E., and Horvitz, H.R. (1993). Odorant-selective genes and neurons mediate olfaction in C. elegans. Cell *74*, 515–527.

Bartel, D.L., Sullivan, S.L., Lavoie, E.G., Sévigny, J., and Finger, T.E. (2006). Nucleoside triphosphate diphosphohydrolase-2 is the ecto-ATPase of type I cells in taste buds. J. Comp. Neurol. *497*, 1–12.

Bermingham-McDonogh, O., Oesterle, E.C., Stone, J.S., Hume, C.R., Huynh, H.M., and Hayashi, T. (2006). Expression of Prox1 during mouse cochlear development. J. Comp. Neurol. *496*, 172–186.

Boettger, T., Hübner, C.A., Maier, H., Rust, M.B., Beck, F.X., and Jentsch, T.J. (2002). Deafness and renal tubular acidosis in mice lacking the K-Cl co-transporter Kcc4. Nature *416*, 874–878.

Breunig, E., Czesnik, D., Piscitelli, F., Di Marzo, V., Manzini, I., and Schild, D. (2010). Endocannabinoid modulation in the olfactory epithelium. Results Probl. Cell Differ. *52*, 139–145.

Chao, M.Y., Komatsu, H., Fukuto, H.S., Dionne, H.M., and Hart, A.C. (2004). Feeding status and serotonin rapidly and reversibly modulate a Caenorhabditis elegans chemosensory circuit. Proc. Natl. Acad. Sci. USA *101*, 15512–15517.

Choksi, S.P., Southall, T.D., Bossing, T., Edoff, K., de Wit, E., Fischer, B.E., van Steensel, B., Micklem, G., and Brand, A.H. (2006). Prospero acts as a binary switch between self-renewal and differentiation in Drosophila neural stem cells. Dev. Cell *11*, 775–789.

Christopherson, K.S., Ullian, E.M., Stokes, C.C., Mullowney, C.E., Hell, J.W., Agah, A., Lawler, J., Mosher, D.F., Bornstein, P., and Barres, B.A. (2005). Thrombospondins are astrocyte-secreted proteins that promote CNS synaptogenesis. Cell *120*, 421–433.

Cuschieri, A., and Bannister, L.H. (1975). The development of the olfactory mucosa in the mouse: electron microscopy. J. Anat. *119*, 471–498.

Doe, C.Q., Chu-LaGraff, Q., Wright, D.M., and Scott, M.P. (1991). The prospero gene specifies cell fates in the Drosophila central nervous system. Cell *65*, 451–464.

Dooley, R., Mashukova, A., Toetter, B., Hatt, H., and Neuhaus, E.M. (2011). Purinergic receptor antagonists inhibit odorant-mediated CREB phosphorylation in sustentacular cells of mouse olfactory epithelium. BMC Neurosci. *12*, 86.

Doroquez, D.B., Berciu, C., Anderson, J.R., Sengupta, P., and Nicastro, D. (2014). A high-resolution morphological and ultrastructural map of anterior sensory cilia and glia in Caenorhabditis elegans. eLife *3*, e01948.

Duerr, J.S., Han, H.P., Fields, S.D., and Rand, J.B. (2008). Identification of major classes of cholinergic neurons in the nematode Caenorhabditis elegans. J. Comp. Neurol. *506*, 398–408.

Dvoryanchikov, G., Sinclair, M.S., Perea-Martinez, I., Wang, T., and Chaudhari, N. (2009). Inward rectifier channel, ROMK, is localized to the apical tips of glial-like cells in mouse taste buds. J. Comp. Neurol. *517*, 1–14.

Elsir, T., Smits, A., Lindström, M.S., and Nistér, M. (2012). Transcription factor PROX1: its role in development and cancer. Cancer Metastasis Rev. *31*, 793–805.

Engström, H. (1967). The ultrastructure of the sensory cells of the cochlea. J. Laryngol. Otol. *81*, 687–715.

Freeman, M.R., and Doe, C.Q. (2001). Asymmetric Prospero localization is required to generate mixed neuronal/glial lineages in the Drosophila CNS. Development *128*, 4103–4112.

Galeeva, A., Treuter, E., Tomarev, S., and Pelto-Huikko, M. (2007). A prospero-related homeobox gene Prox-1 is expressed during postnatal brain development as well as in the adult rodent brain. Neuroscience *146*, 604–616.

Gibbs, G.M., Roelants, K., and O'Bryan, M.K. (2008). The CAP superfamily: cysteine-rich secretory proteins, antigen 5, and pathogenesis-related 1 proteins–roles in reproduction, cancer, and immune defense. Endocr. Rev. *29*, 865–897.

Guenin, L., Raharijaona, M., Houlgatte, R., and Baba-Aissa, F. (2010). Expression profiling of prospero in the Drosophila larval chemosensory organ: Between growth and outgrowth. BMC Genomics *11*, 47.

Hansel, D.E., Eipper, B.A., and Ronnett, G.V. (2001). Neuropeptide Y functions as a neuroproliferative factor. Nature *410*, 940–944.

Hegg, C.C., Irwin, M., and Lucero, M.T. (2009). Calcium store-mediated signaling in sustentacular cells of the mouse olfactory epithelium. Glia *57*, 634–644.

Kamath, R.S., and Ahringer, J. (2003). Genome-wide RNAi screening in Caenorhabditis elegans. Methods *30*, 313–321.

Kimura, K.D., Miyawaki, A., Matsumoto, K., and Mori, I. (2004). The C. elegans thermosensory neuron AFD responds to warming. Curr. Biol. *14*, 1291–1295.

Kolotuev, I., Hyenne, V., Schwab, Y., Rodriguez, D., and Labouesse, M. (2013). A pathway for unicellular tube extension depending on the lymphatic vessel determinant Prox1 and on osmoregulation. Nat. Cell Biol. *15*, 157–168.

Law, C.W., Chen, Y., Shi, W., and Smyth, G.K. (2014). voom: Precision weights unlock linear model analysis tools for RNA-seq read counts. Genome Biol. *15*, R29.

Lawton, D.M., Furness, D.N., Lindemann, B., and Hackney, C.M. (2000). Localization of the glutamate-aspartate transporter, GLAST, in rat taste buds. Eur. J. Neurosci. *12*, 3163–3171.

Leclerc, S., Heydel, J.M., Amossé, V., Gradinaru, D., Cattarelli, M., Artur, Y., Goudonnet, H., Magdalou, J., Netter, P., Pelczar, H., and Minn, A. (2002). Glucuronidation of odorant molecules in the rat olfactory system: activity, expression and age-linked modifications of UDP-glucuronosyltransferase isoforms, UGT1A6 and UGT2A1, and relation to mitral cell activity. Brain Res. Mol. Brain Res. *107*, 201–213.

Liégeois, S., Benedetto, A., Michaux, G., Belliard, G., and Labouesse, M. (2007). Genes required for osmoregulation and apical secretion in Caenorhabditis elegans. Genetics *175*, 709–724.

Love, M.I., Huber, W., and Anders, S. (2014). Moderated estimation of fold change and dispersion for RNA-seq data with DESeq2. Genome Biol. *15*, 550.

Manning, L., and Doe, C.Q. (1999). Prospero distinguishes sibling cell fate without asymmetric localization in the Drosophila adult external sense organ lineage. Development *126*, 2063–2071.

Matsunobu, T., Chung, J.W., and Schacht, J. (2001). Acetylcholine-evoked calcium increases in Deiters' cells of the guinea pig cochlea suggest alpha9-like receptors. J. Neurosci. Res. *63*, 252–256.

Murray, R.G. (1993). Cellular relations in mouse circumvallate taste buds. Microsc. Res. Tech. *26*, 209–224.

Oikonomou, G., and Shaham, S. (2011). The glia of Caenorhabditis elegans. Glia *59*, 1253–1263.

Oikonomou, G., Perens, E.A., Lu, Y., Watanabe, S., Jorgensen, E.M., and Shaham, S. (2011). Opposing activities of LIT-1/NLK and DAF-6/patched-related direct sensory compartment morphogenesis in C. elegans. PLoS Biol. *9*, e1001121.

Papanayotou, C., De Almeida, I., Liao, P., Oliveira, N.M., Lu, S.Q., Kougioumtzidou, E., Zhu, L., Shaw, A., Sheng, G., Streit, A., et al. (2013). Calfacilitin is a calcium channel modulator essential for initiation of neural plate development. Nat. Commun. *4*, 1837.

Parrish, S., and Fire, A. (2001). Distinct roles for RDE-1 and RDE-4 during RNA interference in Caenorhabditis elegans. RNA *7*, 1397–1402.

Peco, E., Davla, S., Camp, D., Stacey, S., Landgraf, M., and van Meyel, D. (2016). *Drosophila* astrocytes cover specific territories of CNS neuropil and are instructed to differentiate by Prospero, a key effector of Notch. Development dev., 133165, Published online February 18, 2016. http://dx.doi.org/10.1242/dev.133165.

Perkins, L.A., Hedgecock, E.M., Thomson, J.N., and Culotti, J.G. (1986). Mutant sensory cilia in the nematode Caenorhabditis elegans. Dev. Biol. *117*, 456–487.

Pistocchi, A., Feijóo, C.G., Cabrera, P., Villablanca, E.J., Allende, M.L., and Cotelli, F. (2009). The zebrafish prospero homolog prox1 is required for mechanosensory hair cell differentiation and functionality in the lateral line. BMC Dev. Biol. *9*, 58.

Robinson, M.D., McCarthy, D.J., and Smyth, G.K. (2010). edgeR: a Bioconductor package for differential expression analysis of digital gene expression data. Bioinformatics *26*, 139–140.

Ryu, W.S., and Samuel, A.D. (2002). Thermotaxis in Caenorhabditis elegans analyzed by measuring responses to defined Thermal stimuli. J. Neurosci. *22*, 5727–5733.

Shaham, S. (2006). Glia-neuron interactions in the nervous system of Caenorhabditis elegans. Curr. Opin. Neurobiol. *16*, 522–528.

Shaham, S. (2010). Chemosensory organs as models of neuronal synapses. Nat. Rev. Neurosci. *11*, 212–217.

Shaham, S. (2015). Glial development and function in the nervous system of Caenorhabditis elegans. Cold Spring Harb. Perspect. Biol. *7*, a020578.

Spencer, W.C., McWhirter, R., Miller, T., Strasbourger, P., Thompson, O., Hillier, L.W., Waterston, R.H., and Miller, D.M., 3rd. (2014). Isolation of specific neurons from C. elegans larvae for gene expression profiling. PLoS ONE *9*, e112102.

Stiernagle, T. (2006). Maintenance of C. elegans. WormBook, 1–11.

Strauss, O. (2005). The retinal pigment epithelium in visual function. Physiol. Rev. *85*, 845–881.

Suh, J., and Hutter, H. (2012). A survey of putative secreted and transmembrane proteins encoded in the C. elegans genome. BMC Genomics *13*, 333.

Tabara, H., Sarkissian, M., Kelly, W.G., Fleenor, J., Grishok, A., Timmons, L., Fire, A., and Mello, C.C. (1999). The rde-1 gene, RNA interference, and transposon silencing in C. elegans. Cell *99*, 123–132.

Trotier, D. (1998). Electrophysiological properties of frog olfactory supporting cells. Chem. Senses *23*, 363–369.

Ward, S. (1973). Chemotaxis by the nematode Caenorhabditis elegans: identification of attractants and analysis of the response by use of mutants. Proc. Natl. Acad. Sci. USA *70*, 817–821.

Winter, E., and Ponting, C.P. (2002). TRAM, LAG1 and CLN8: members of a novel family of lipid-sensing domains? Trends Biochem. Sci. *27*, 381–383.

Yan, N. (2015). Structural Biology of the Major Facilitator Superfamily Transporters. Annu. Rev. Biophys. *44*, 257–283.

Zhang, S., and Kuhn, J.R. (2013). Cell isolation and culture. WormBook, 1–39.

Zhang, Y., Chen, K., Sloan, S.A., Bennett, M.L., Scholze, A.R., O'Keeffe, S., Phatnani, H.P., Guarnieri, P., Caneda, C., Ruderisch, N., et al. (2014). An RNA-sequencing transcriptome and splicing database of glia, neurons, and vascular cells of the cerebral cortex. J. Neurosci. *34*, 11929–11947.